

Synthesis of Single-Crystal CdS Microbelts Using a Modified Thermal Evaporation Method and Their Photoluminescence

Guozhen Shen,^{*,†,‡} Jung Hee Cho,[†] Jin Kyoung Yoo,[§] Gyu-Chul Yi,[§] and Cheol Jin Lee^{*,†}

Department of Nanotechnology, Hanyang University, 17 Haengdang-dong, Seongdong-gu, Seoul 133-791, South Korea, and Department of Materials Science and Engineering, Pohang University of Science and Technology, San-31 Hyoja-dong, Pohang 790-784, South Korea

Received: November 8, 2004; In Final Form: February 28, 2005

Large-scale synthesis of single-crystal CdS microbelts was achieved by a modified thermal evaporation method, in which an adiabatic layer was used to provide abrupt temperature decrease and high gas concentration for the microbelt growth. The synthesized CdS microbelts were usually several micrometers in width, 70 nm in thickness, and tens to several hundred micrometers in length. Studies found that the adiabatic layer has great influence on the formation of CdS microbelts. Room-temperature photoluminescence indicated the disappearance of the emission at 1.77 eV, the appearance of an emission at 2.07 eV, and also the enhancement of the emission band at 2.38 eV, whose position shifted toward the blue region compared with conventional narrow CdS nanobelts. A possible growth mechanism of the CdS microbelts was briefly discussed.

1. Introduction

In recent years, intensive research has been conducted on one-dimensional (1D) nanostructures of semiconductors, owing to their fundamental significance for studying the dependence of various physical properties on dimensionality and size reduction as well as the potential for applications in nanodevices.^{1,2} Previous research has mainly focused on the investigation of nanotubes, nanorods, and nanowires including the development of synthetic methods and studies on their novel physical properties.^{3–6} Very recently, another interesting configuration of 1D growth, called nanobelts, has been discovered first for metal oxides.⁷ In nanobelts, the thickness of the belt is much smaller than its width, such that the confinement is far from uniform in the cross section as compared to its nanowire counterparts. This unique structure not only helps to extend the understanding of structure–property relationships in solids but can also contribute to an ideal system for building functional devices. Since its discovery, several strategies have been developed for the preparation of nanobelts, including chemical or physical vapor deposition^{7–14} organogel-template-directed growth,¹⁵ hydrothermal growth,^{16,17} and so on. Unfortunately, most of the reported nanobelts were very narrow, usually tens to several hundred nanometers in width. Due to investigating their intriguing properties and their potential applications to nanoscale devices, exploring nanobelts with very large widths on the micrometer scale, in other words, microbelts, still remains significant.

CdS is one of the most important II–VI semiconductors. It is an important direct-band semiconductor with a band gap of 2.4 eV. CdS has vital optoelectronic applications for laser light-emitting diodes and optical devices based on nonlinear proper-

ties.¹⁹ Though several techniques have been used to synthesize CdS nanobelts, usually extremely low pressure, special procedures to avoid the oxidation of the substrate are needed, and all of the reported CdS nanobelts are very narrow in width, only tens to several hundred nanometers.^{14,18}

In this work, we report the large-scale synthesis of high-quality CdS microbelts using a simple modified thermal evaporation process. To obtain the CdS microbelts, an adiabatic layer was used. The typical widths of the as-synthesized CdS microbelts were several to 10 μm , which is much wider than previously reported CdS nanobelts.^{14,18} Room-temperature photoluminescence (PL) studies of the CdS microbelts indicated the disappearance of the emission at 1.77 eV, the appearance of an emission at 2.07 eV, and also the enhancement of the emission band at 2.38 eV, whose position shifted toward the blue region as compared with conventional narrow CdS nanobelts.

2. Experimental Section

The fabrication process is based on an atmospheric pressure thermal evaporation of CdS nanoparticles in the presence of Au catalyst. A quartz tube was mounted horizontally inside a high-temperature tube furnace. Approximately 0.2 g of the CdS nanoparticles (self-made by refluxing $\text{Cd}(\text{NO}_3)_2$ and thiourea in ethylene glycol according to the literature²¹) was placed in the center of the tube. A layer of gold thin film (~ 20 nm) was first deposited on the silicon wafer using a sputtering method. And then the silicon substrate was placed downstream in the tube (10 cm away from source material). To get microbelts, an adiabatic layer with length of about 10 cm was used to ensure the abrupt temperature decrease. Prior to being heated, the system was flushed with high-purity Ar for 10 min to eliminate O_2 . Then under a constant flow of Ar (200 sccm), the furnace was rapidly heated to 900 $^\circ\text{C}$, held at this temperature for about 1 h, and subsequently cooled to room temperature. The general morphology of the products was examined by scanning electron microscopy (SEM, Hitachi S-4700). Powder X-ray diffraction (XRD, Rigaku DMAX 2500) was employed to examine their

* Authors to whom correspondence should be addressed. Phone: +82-2-2293-4744 (G.S.). Fax: +82-2-2290-0768 (G.S.). E-mail: gzshen@ustc.edu; cjlee@hanyang.ac.kr.

[†] Hanyang University.

[‡] Present address: Advanced Materials Laboratory, National Institute for Materials Science (NIMS), 1-1 Namiki, Tsukuba, Ibaraki 305-0044, Japan.

[§] Pohang University of Science and Technology.

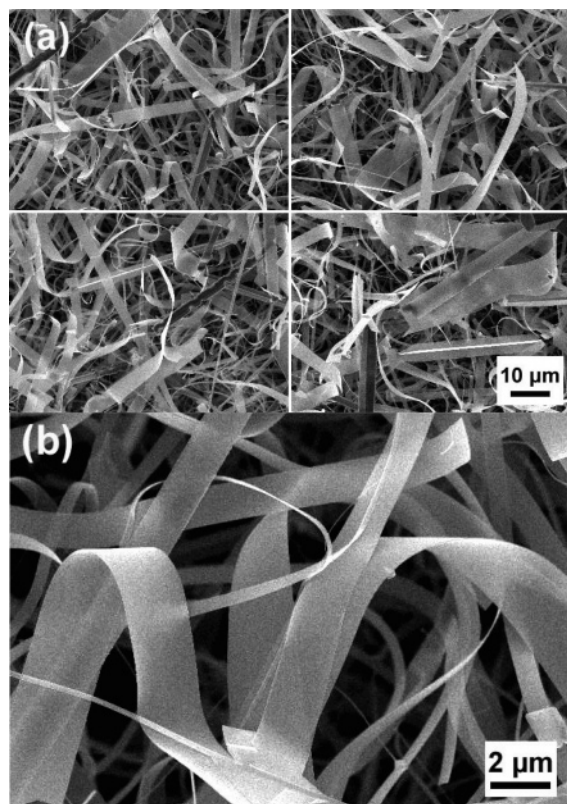


Figure 1. (a) SEM images of as-deposited CdS microbelts. (b) High-magnification SEM image clearly revealing the beltlike morphology.

overall crystallinity. The chemical composition analysis was achieved by energy-dispersive X-ray spectrometry (EDX, Hitachi S-4700), using an EDX spectrometer attached to the SEM. The detailed microstructure analysis was carried out using high-resolution transmission electron microscopy (HRTEM, JEOL JEM 3011 and JEOL JEM 2010). Photoluminescence (PL) studies of the microbelts were performed at room temperature with an optical resolution of 0.02–0.1 nm, and the 442 nm line of a continuous-wave He–Cd laser was used as the excitation source.

3. Results and Discussion

After the reaction, it was found that many yellow cottonlike fibers appeared on the surface of the silicon substrate and the source material (CdS nanoparticles) was depleted. Figure 1a shows the SEM image of the as-synthesized products on the Au-coated silicon substrate. The products consist of a large quantity of beltlike nanostructures with typical lengths of tens to several hundred micrometers and widths up to 10 μm. A highly magnified SEM image (Figure 1b) shows several twisted "belts", which clearly reveal the microbelt-like morphology.⁷ The thickness of each microbelt is quite thin, about 70 nm.

The phase composition of as-synthesized products was examined by EDX. Figure 2a shows the EDX spectra of the sample, which indicates that the microbelts consist of only Cd and S. Figure 2b is the typical XRD pattern of the CdS products deposited on the silicon substrate. All of the strong and sharp peaks of the XRD pattern can be readily indexed to the hexagonal structure of CdS with calculated lattice constants $a = 4.131 \text{ \AA}$ and $c = 6.702 \text{ \AA}$, consistent with the standard literature values of $a = 4.136 \text{ \AA}$ and $c = 6.713 \text{ \AA}$ (Joint Committee on Powder Diffraction Standards Card. No. 77-2306). The peak marked with a star comes from catalyst Au on the substrate.

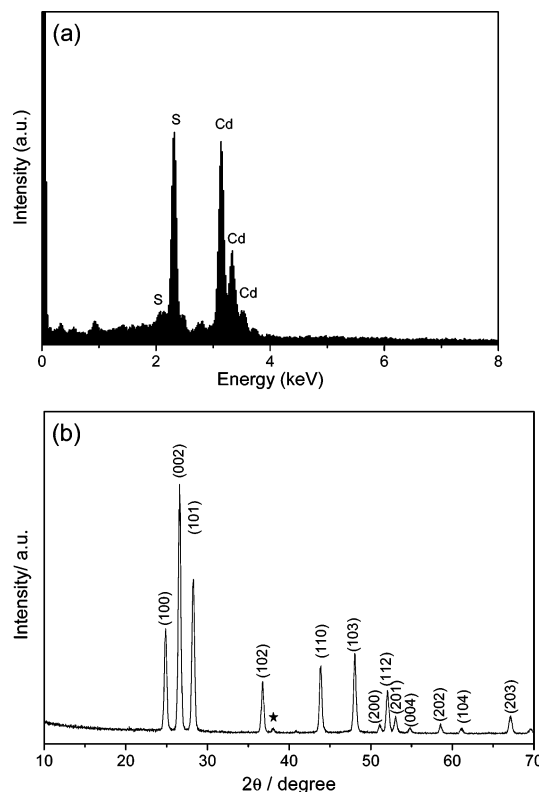


Figure 2. (a) EDX and (b) XRD patterns of the deposited CdS microbelts, showing the formation of the pure CdS product.

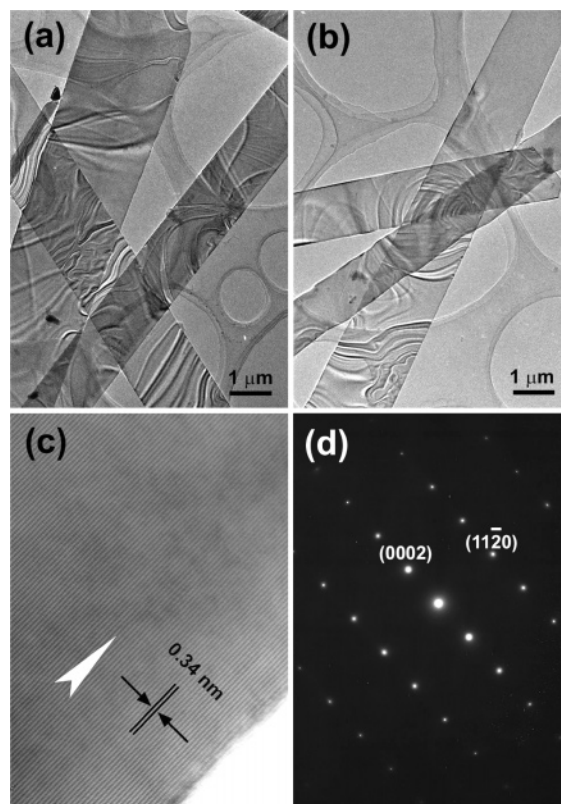


Figure 3. (a and b) TEM images showing several CdS microbelts. (c) a HRTEM image of the CdS microbelt grown along the [11–20] direction. (d) Corresponding SAED pattern of the microbelt shown in part c.

Further structural analysis was performed using HRTEM (JEOL JEM 3011). Figures 3a and 3b are the low-magnification TEM images of the CdS microbelts synthesized by the

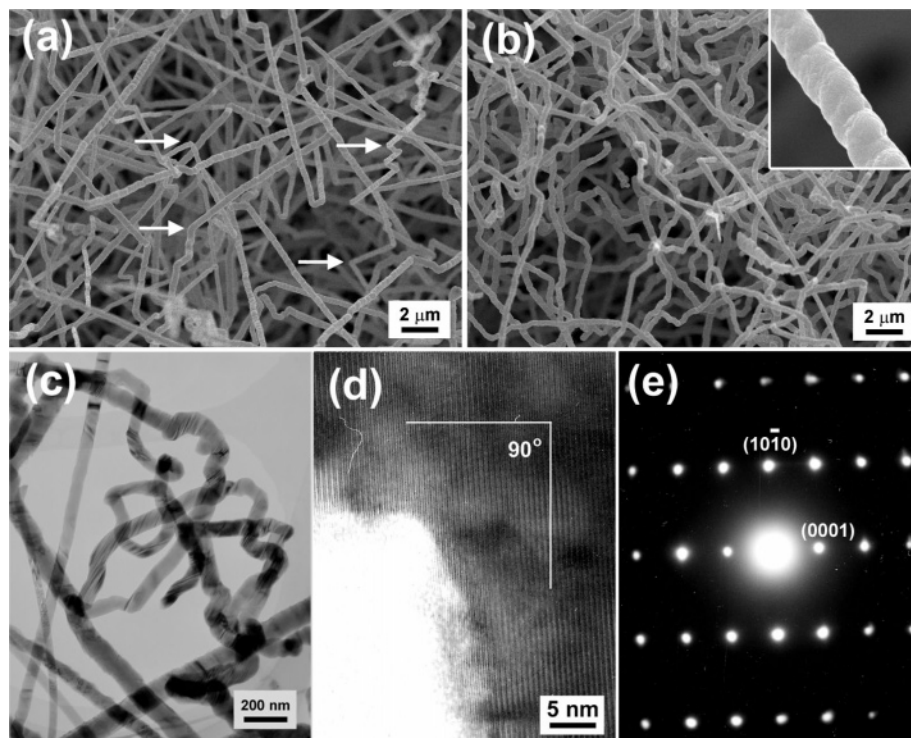


Figure 4. (a and b) SEM images, (c) TEM image, (d) HRTEM image, and (e) SAED pattern of the product synthesized at 800 °C, showing the formation of zigzag CdS nanowires.

atmospheric pressure thermal evaporation process, which show the general morphology of the as-synthesized microbelts dispersed on the carbon film. Each microbelt has a very smooth surface without any sheathed amorphous layer and has a uniform width along its entire length. It was found that the microbelts are almost transparent; the copper grid can even be clearly seen through the thin microbelts. The ripplelike contrast in the TEM images may be due to the strain resulting from the belt bending. Several TEM images of the cross section show that it has a rectangular-like cross section. Insight into the structure of the microbelts can be revealed by HRTEM in Figure 3c. The d spacing of 0.34 nm corresponds well to the (0002) plane of CdS. And the corresponding selected area electron diffraction (SAED) pattern (Figure 3d) demonstrates the [11–20] crystalline direction as the growth direction of the CdS microbelts. From the HRTEM examination, it was found that no dislocation and planar defects, such as stacking faults and twins, exist in the microbelts.

The growth mechanism of nanobelts or microbelts generally depends on the presence or absence of metal catalysts in the synthesis process, i.e., vapor–liquid–solid (VLS) and vapor–solid (VS) mechanisms.²² The formation of the CdS microbelts may relate to the VLS mechanism, as supported by several experimental observations. (1) From SEM and TEM observations, droplets are indeed observed at the tips of the microbelts, which is evidence for the VLS mechanism; (2) thermal evaporation of the CdS nanoparticles without Au at the same experimental condition results in the CdS multipod-based structures on the substrate.²³ During thermal evaporation of the CdS nanoparticles, the Au thin film is annealed to form liquid Au particles. Evaporated CdS vapor is rapidly generated at relatively high temperature, and then it is transferred to the low-temperature region by the Ar carrier gas where it reacts with the Au liquid to form alloy droplets. As CdS in the droplets becomes supersaturated, CdS microbelts will be formed by precipitation at the liquid/solid interface.

Even though the VLS mechanism is responsible for the formation of the CdS microbelts, it must be pointed out that the growth process of the microbelts may be quite different from the conventional VLS mechanism, in which the size of the nanowires is confined by the size of the catalyst particles, because if the reaction is controlled by the conventional VLS mechanism, CdS microrods or nanorods should be formed instead of the CdS microbelts. In the current studies, it was thought that Au may only be involved during the physical absorption process rather than further contributing to the 1D growth just as in the previous report.¹⁴ Obviously, parameters that affect the crystal growth kinetics, such as reaction temperature, may also play an important role in determining microbelt morphology. At a suitable temperature, the CdS microbelts will grow along specific directions, and their surfaces are defined by specific crystallographic planes. This suggestion was supported by the fact that thermal evaporation of the CdS nanoparticles at low temperature (800 °C) contributes to only nanowires just as in the previous report.²⁴ This is consistent with previous reports concerning the growth of nanowires and nanobelts, in which the nanobelt growth prefers higher-temperature conditions.^{7,14} Figures 4a and 4b show the SEM images of the obtained CdS nanowires at 800 °C, which indicate that the CdS nanowires have diameters of 80–150 nm and their lengths are up to several hundred micrometers. In comparison with the previous report on CdS nanowires,²⁴ the CdS nanowires produced by the present modified thermal evaporation method indicate curved morphology and rough surfaces (Figure 4b, inset). Some zigzag CdS nanowires are clearly presented as shown in Figure 4a (white arrows). The TEM image of the CdS nanowires shown in Figure 4c confirms the formation of curved CdS nanowires. Further structural analysis using HRTEM (JEOL JEM 2010) and SAED shown in Figures 4d and 4e indicates the single-crystal nature of the CdS nanowires. And further studies on the structural and other properties of the curved CdS nanowires are still underway in our group.

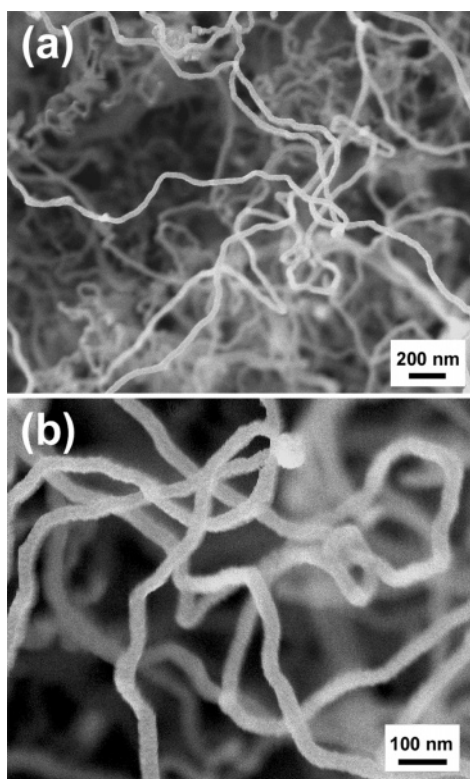


Figure 5. SEM images of SiO₂ nanowires synthesized in the conventional chemical vapor deposition system.

In our experiments, the use of the adiabatic layer is the critical reason for the formation of the CdS microbelts. Without the adiabatic layer, only SiO₂ nanowires were formed on the substrate. Figure 5 shows the SEM images of the obtained SiO₂ nanowires without the use of the adiabatic layer in the system. It indicates that the SiO₂ nanowires have diameters of about 30 nm and lengths of several hundred micrometers. Catalyst particles are detected at the tips of several SiO₂ nanowires, revealing the VLS growth mechanism for the formation of SiO₂ nanowires. The formation of SiO₂ nanowires is due to the oxidation of the silicon substrate at high temperature just as in the previous report.¹⁴ Though the function of the adiabatic layer in the formation of the CdS microbelts is still unclear, it is undoubtable that the use of the adiabatic layer has a great influence on the formation of the CdS microbelts according to the above analyses. Since thermal evaporation of the CdS nanoparticles at different temperatures resulted in different CdS products, it is reasonable to think that the formation of microbelt structures is mainly controlled by two factors as in the previous reports on nanobelts. The surface energy determines the preferential surfaces that will grow, whereas the growth kinetics determines the final structure. On the basis of these results, it was thought that the use of the adiabatic layer is suitable for the formation of the CdS microbelts mainly due to the following two factors. One is that it provides an abrupt decrease of the silicon substrate temperature and thus avoids the oxidation of the silicon substrate, but the temperature is still high enough to ensure the formation of the beltlike morphology instead of the wirelike morphology. The other is that the existence of the adiabatic layer near the source material ensures a high concentration of CdS gas near the substrate for the formation of microbelts. And more experiments are undoubtedly required to further investigate the influence of the adiabatic layer.

The room-temperature PL measurement results of the CdS microbelts are shown in Figure 6a. It is clear that the spectrum

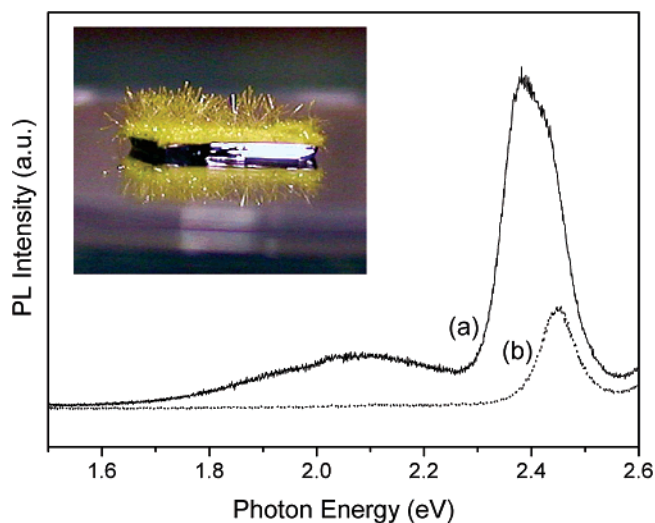


Figure 6. Room-temperature PL spectra of (a) CdS microbelts and (b) CdS microrods synthesized in the improved thermal evaporation process.

consists of a sharp and strong emission band located at 2.38 eV and a weak and broad emission band centered at 2.07 eV. In the past several years, the luminescence mechanisms of one-dimensional CdS nanostructures have been extensively studied. Usually, two emissions are observed from semiconductor nanostructures, excitonic and trapped luminescence, respectively. Zhao et al. reported the PL properties of multiarmed CdS nanorods, and one-emission peak centered at about 710 nm was observed, which came from a self-activated emission of CdS.²⁵ Li et al. reported that two emission bands were observed in the PL spectra of CdS nanowires.²⁶ In their result, the band at 519 nm corresponds to the band gap of CdS while the other at 620 nm is attributed to an internal defect emission. Liu et al. have reported the PL spectrum of narrow CdS nanobelts consisting of one weak emission at 517 nm and another strong and broad emission at 735 nm.²⁷ Therefore, it is suggested that the luminescence at 2.38 eV observed from the CdS microbelts originates from the recombination of free excitons and the emission at 2.07 eV can be attributed to deep levels associated with sulfur vacancies, extrinsic defects, or impurities.

The difference in optical properties for different shapes and phase structures of the semiconductor nanocrystals has attracted significant attention recently,^{28–30} so comparison with the optical properties of the CdS microrods and narrow nanobelts may help us better understand the intrinsic PL properties of our deposited CdS microbelts. Figure 6b is the PL spectra of the CdS microrods, which shows only a strong emission at 2.45 eV. The CdS microrods were prepared in a similar process except that the deposited substrate was put directly next to the source materials (the distance between source materials and substrate was 0.5–1 cm). The inset in Figure 6 shows the optical image of the obtained CdS microrods. From these spectra, we can see that PL emission of the CdS microbelts became much stronger than that of CdS microrods and the emission band shows a blue shift of about 0.07 eV compared with the CdS microrods.

Figure 7 shows the PL spectra for both the CdS microbelts and the CdS nanobelts at room temperature. The CdS nanobelts are obtained by a catalyst-free vapor transport process similar to the report of Zhang et al. (The inset of Figure 7 shows the SEM image of the CdS nanobelts.¹⁸) In comparison with the spectra of the CdS microbelts (Figure 7a), the intensity of the emission peak of the CdS nanobelts is much weaker. Furthermore, the peak of the CdS microbelts also shifts to a lower

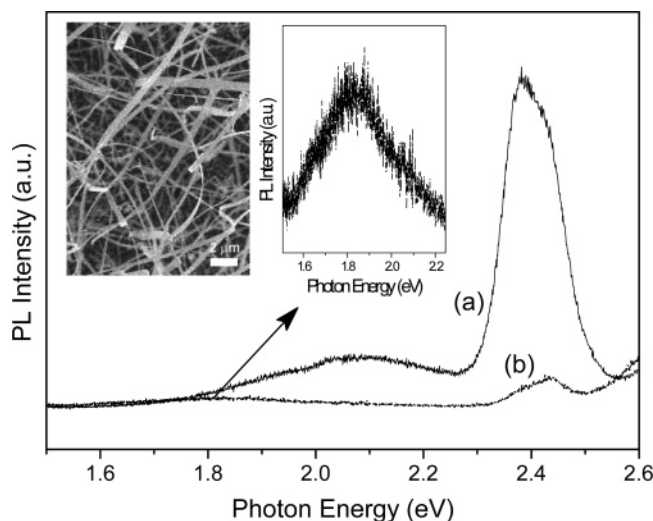


Figure 7. PL spectra of (a) CdS microbelts from the improved thermal evaporation process and (b) CdS nanobelts from the conventional thermal evaporation process.

energy due to their special structural properties. For the internal defect emission, a weak peak centered at 1.77 eV was observed for the CdS nanobelts and at 2.07 eV for the CdS microbelts, respectively. This difference is also related to the special structure and surface properties of the CdS microbelts, and the results are consistent with previous reports of the relationship between the morphology and the optical properties on nanostructures.^{28–30}

4. Conclusion

We demonstrated the large-scale synthesis of CdS microbelts with typical widths of several micrometers using a modified thermal evaporation method. Most of the CdS microbelts were several micrometers in diameter, had smooth and clean surfaces, and also indicated the [11–20] growth direction. Room-temperature PL spectra of the microbelts revealed a strong emission band at 2.38 eV and a weak and broad emission band at 2.07 eV, quite different from those of the CdS microrods and narrow CdS nanobelts. The growth of the CdS microbelts is controlled by the thermodynamics of crystal growth involving different facets. The use of the adiabatic layer not only avoids the oxidation of the substrate but also provides a high gas concentration for the formation of CdS microbelts.

Acknowledgment. This work was supported by Center for Nanotubes and Nanostructured Composites at SKKU, by the National R&D Project for Nano Science and Technology of

MOST. G.S. thanks Professor Tang at the Hefei National Laboratory for Physical Science at the Microscale for his great help on the analysis of the SAED and HRTEM images.

References and Notes

- (1) Xia, Y. N.; Yang, P. D.; Sun, Y. G.; Wu, Y. Y.; Mayers, B.; Gates, B.; Yin, Y. D.; Kim, F.; Yan, H. Q. *Adv. Mater.* **2003**, *15*, 353.
- (2) Rao, C. N. R.; Gundiah, G.; Deepark, F. L.; Govindaraj, A.; Cheetham, A. K. *J. Mater. Chem.* **2004**, *14*, 440.
- (3) Zhang, Y.; Suenaga, K.; Colliex, C.; Iijima, S. *Science* **1998**, *281*, 973.
- (4) Li, Y. D.; Wang, J. W.; Deng, Z. X.; Wu, Y. Y.; Sun, X. M.; Yu, D. P.; Yang, P. D. *J. Am. Chem. Soc.* **2001**, *123*, 9904.
- (5) Jo, S. H.; Lao, J. Y.; Ren, Z. F.; Farrer, R. A.; Baldacchini, T.; Foukas, J. T. *Appl. Phys. Lett.* **2003**, *83*, 4821.
- (6) Wang, Y. W.; Meng, G. W.; Zhang, L. D.; Liang, C. H.; Zhang, J. *Chem. Mater.* **2002**, *14*, 1773.
- (7) Pan, Z. W.; Dai, Z. R.; Wang, Z. L. *Science* **2001**, *291*, 1947.
- (8) Bae, S. Y.; Seo, H. W.; Park, J.; Yang, H.; Park, J. C.; Lee, S. Y. *Appl. Phys. Lett.* **2002**, *81*, 126.
- (9) Wu, Q.; Hu, Z.; Wang, X. Z.; Chen, Y.; Lu, Y. N. *J. Phys. Chem. B* **2003**, *107*, 9726.
- (10) Fu, L.; Liu, Y. Q.; Hu, P.; Xiao, K.; Yu, G.; Zhu, D. B. *Chem. Mater.* **2003**, *15*, 4287.
- (11) Cao, X. B.; Xie, Y.; Zhang, S. Y.; Li, F. Q. *Adv. Mater.* **2004**, *16*, 649.
- (12) Jiang, Y.; Meng, M. X.; Liu, J.; Xie, Z. Y.; Lee, C. S.; Lee, S. T. *Adv. Mater.* **2003**, *15*, 323.
- (13) Li, Q.; Wang, C. R. *Appl. Phys. Lett.* **2003**, *83*, 359.
- (14) Dong, L. F.; Jiao, J.; Coulter, M.; Love, L. *Chem. Phys. Lett.* **2003**, *376*, 653.
- (15) Jung, J. H.; Kobayashi, H.; Van Bommel, K. J. C.; Shinkai, S.; Shimizu, T. *Chem. Mater.* **2002**, *14*, 1445.
- (16) Mo, M. S.; Zeng, J. H.; Liu, X. M.; Yu, W. C.; Zhang, X. Y.; Qian, Y. T. *Adv. Mater.* **2002**, *14*, 1658.
- (17) Yu, J. G.; Yu, J. C.; Ho, W. K.; Wu, L.; Wang, X. C. *J. Am. Chem. Soc.* **2004**, *126*, 3422.
- (18) Zhang, J.; Jiang, F.; Zhang, L. D. *J. Phys. Chem. B* **2004**, *108*, 7002.
- (19) Weinhardt, L. *Appl. Phys. Lett.* **2003**, *82*, 571.
- (20) Li, Y. D.; Liao, H. W.; Ding, Y.; Fan, Y.; Zhang, Y.; Qian, Y. T. *Inorg. Chem.* **1999**, *38*, 1382.
- (21) Shen, G. Z.; Chen, D.; Tang, K. B.; Liu, X. M.; Huang, L. Y.; Qian, Y. T. *J. Solid State Chem.* **2003**, *173*, 232.
- (22) Wang, Z. L. *Adv. Mater.* **2003**, *15*, 432.
- (23) Shen, G. Z.; Lee, C. J. *Cryst. Growth Des.*, in press.
- (24) Wang, Y. W.; Meng, G. W.; Zhang, L. D.; Liang, C. H.; Zhang, J. *Chem. Mater.* **2004**, *14*, 1773.
- (25) Gao, F.; Lu, Q. Y.; Xie, S. H.; Zhao, D. Y. *Adv. Mater.* **2002**, *14*, 1537.
- (26) Ge, J. P.; Li, Y. D. *Adv. Funct. Mater.* **2004**, *14*, 157.
- (27) Liu, W. F.; Jin, C. G.; Jia, C.; Yao, L. Z.; Cai, W. L.; Li, X. G. *Chem. Lett.* **2004**, *33*, 228.
- (28) Djuricic A. B.; Leung, Y. H.; Choy, W. C. H.; Cheah, K. W.; Chan, W. K. *Appl. Phys. Lett.* **2004**, *84*, 2635.
- (29) Shalish, I.; Temkin, H.; Narayanamurti, V. *Phys. Rev. B* **2004**, *69*, 245401.
- (30) Krishnamachari, U.; Borgstrom, M.; Ohlsson, B. J.; Panev, N.; Samuelson, L.; Seifert W.; Larsson, M. W.; Wallenberg, L. R. *Appl. Phys. Lett.* **2004**, *85*, 2077.